Environ. Sci. Technol. **2003**, *37,* 3755−3763

Gaseous Elemental Mercury in the Marine Boundary Layer: Evidence for Rapid Removal in Anthropogenic Pollution

PETER WEISS-PENZIAS,*
DANIEL A. JAFFE, AND
ANNA MCCLINTICK

Interdisciplinary Arts and Sciences, University of Washington−Bothell, 18115 Campus Way NE, Bothell, Washington 98011

ERIC M. PRESTBO

Frontier Geosciences, 414 Pontius Avenue N, Seattle, Washington 98109

MATTHEW S. LANDIS

U.S. EPA, Office of Research and Development, Research Triangle Park, North Carolina 27711

In this study, gas-phase elemental mercury (Hg^0) and related species (including inorganic reactive gaseous mercury (RGM) and particulate mercury (PHg)) were measured at Cheeka Peak Observatory (CPO), Washington State, in the marine boundary layer during 2001−2002. Air of continental origin containing anthropogenic pollutants from the urban areas to the east contained on average 5.3% lower Hg^0 levels as compared to the marine background. This result is difficult to reconcile since it is known that industrial emissions in our region are sources of Hg^0. The rate of removal of Hg^0 from a pollution plume necessary to account for our observations is inconsistent with the accepted view of Hg^0 as a stable atmospheric pollutant. The largest and most frequent Hg^0 loss events occurred in the presence of increased ozone (O_3) during the summer. Hg^0 and O_3 also display diurnal cycles that are out-of-phase with one another. In other seasons Hg^0 behavior is less consistent, as we observe weak positive correlations with O_3 and occasional Hg^0 enhancements in local pollution. RGM and PHg concentrations are enhanced only slightly during Hg^0 loss events, comprising a small fraction of the mercury pool (∼3%). Long-range transported pollution of Asian origin was also detected at CPO, and this contains both higher and lower levels of Hg^0 as compared to the background with maximum changes being <20%. Here, the more photochemically processed the air mass, as determined by propane/ethane ratios, the more likely we are to observe Hg^0 loss. Air from the marine background in summer displays a significant diurnal cycle with a phase that matches the diurnal cycles seen in polluted air masses. A Junge lifetime for Hg^0 in the clean marine boundary layer is calculated to be 7.1 months, which is on the low end of previous estimates (0.5−2 yr).

* Corresponding author phone: (425)352-3475; fax: (425)352-5335; e-mail: pweiss@uwb.edu.

Introduction

Mercury (Hg) is a persistent and toxic element with an ability to become methylated and bioaccumulated in aquatic ecosystems. Human exposure to contaminated fish and marine mammals represents a public health concern on a global scale (*1*). The atmosphere has been identified as an important cycling pathway in the global distribution of Hg (*2*−*4*). This stems from the fact that elemental gaseous Hg (Hg^0) is the dominant form in the atmosphere (>95%) and has a sufficiently long lifetime of 0.5−2 yr to allow transport far from source regions. Inorganic divalent Hg (or reactive gaseous Hg, RGM) and particulate-phase Hg (PHg) are also present but have much shorter atmospheric lifetimes than the elemental form because they deposit via wet and dry processes much more rapidly (*4*). Natural sources, including the oceans, crustal outgassing, and volcanoes, emit predominantly Hg^0 (*5*, *6*). Anthropogenic sources such as coal combustion, waste incineration, and cement production release large amounts of RGM and PHg in addition to Hg^0 (*7*). Globally, it is estimated that up to 80% of the present Hg emissions to the atmosphere are of anthropogenic origin (*8*). As a result, total deposition of Hg has increased by a factor of 2−20 since preindustrial times (*9*−*11*).

Anthropogenic emissions of Hg are decreasing in Europe (*7*, *12*) and North America (*13*), which has resulted in a flat or decreasing trend in Hg^0 concentrations since the mid-1990s (*14*−*17*). However, because of the large amounts of coal burned in East Asia presently (*18*) and projected into the future (*19*), there are concerns that global Hg emissions may still be increasing (*20*).

While Hg^0 is generally considered to be long-lived, conversion to RGM and subsequent removal from the atmosphere on a time scale of hours to days has been observed in the polar regions. During polar sunrise, it appears that reactive halogen species, released from the ice pack due to the accumulation of sea salt, cause rapid losses in Hg^0 and ozone (*21*−*23*). During the Antarctic summer, however, Hg^0 losses are associated with ozone increases (*24*). Reaction with OH (*25*) has been proposed to be the dominant Hg^0 removal mechanism in this case, as high OH levels may result from enhanced HONO concentrations due to photodenitrification processes in the snowpack (*24*). There is no evidence, however, that these mechanisms are an important Hg^0 removal pathway in the midlatitudes.

The influence of long-range transport of industrial pollutants, dust, and biomass burning emissions to the west coast of North America has been well-documented (*26*−*28*). Thus, one of the goals of this work is to better understand the relative contributions of local and long-range transported Hg to a remote location on the west coast of North America, where there has been a paucity of measurements. Additionally, the reactivity of Hg^0 is investigated, which suggests that Hg^0 is much less stable in local anthropogenic pollution than was previously thought.

Site and Methods

Measurements were made at the Cheeka Peak Observatory (CPO) in Washington State (48.3 N, 124.6 W, 480 m above sea level), shown in Figure 1. This site is located on the northwestern tip of the Olympic Peninsula, immediately adjacent to the Pacific Ocean, and is usually in the marine boundary layer (MBL). This site has been used for atmospheric chemistry and aerosol research for approximately 15 yr (*27*, *29*). During westerly flow, the air masses that arrive at the site are generally unaffected by recent North American

10.1021/es0341081 CCC: $25.00
Published on Web 07/26/2003

FIGURE 1. Location of Cheeka Peak Observatory (CPO) on the western tip of the contiguous United States. Also shown are the locations of the major urban areas that could influence CPO during continental air flow conditions.

emissions (with the exception of ship emissions) and are characteristic of the North Pacific atmosphere (*27*, *29*). Easterly winds bring air from the more polluted Vancouver–Seattle corridor, which is approximately 150 km to the east. Anthropogenic Hg sources in Washington State are estimated at 2.5 t annually (*30*). Over a 2-yr period (1994–1995), the average total Hg (Hg^0 + RGM + PHg) concentration in the Seattle metro area was measured at 2.5 ng/m^3 (*31*), which is higher than the approximate Northern Hemisphere background of 1.7 ng/m^3 (*16*), presumably due to regional sources.

Air masses were classified as either "continental" or "marine" based on back trajectories using the NOAA-CMDL isentropic model (*32*) or the HYSPLIT model from NOAA-ARL (*33*, *34*). Wind directions between 160° and 315° and wind speeds >2 m/s were also used in classifying air masses as marine. Marine air masses occurred over 50% of the time except during the winter, when the occurrence went down to 43% due to a greater frequency of easterly winds.

Hg^0, CO, O_3, and meteorological parameters were measured nearly continuously from May 2001 to May 2002. RGM measurements began in September 2001, and PHg was measured during selected times throughout the campaign. Radon, aerosol light-scattering, and nonmethane hydrocarbon measurements were added in March 2002 as part of the Intercontinental Transport and Chemical Transformation 2002 (ITCT 2k2) campaign (*35*).

CO was measured with a commercial nondispersive infrared absorbance instrument (API-300, Advanced Pollution Instruments, San Diego, CA) modified to reduce water vapor interference and improve detection limits (*36*). O_3 was measured with a standard UV absorption technique (Dasibi 1008 RS, Glendale, CA). During this study, these instruments were calibrated identically as in our previous work (*27*). The uncertainty for the CO and O_3 hourly averages is estimated to be 6% and 2%, respectively (*27*). Radon (Rn) gas was measured by collection of its daughter products on a filter (*37*). Aerosol light-scattering measurements were made with a single wavelength integrating nephelometer (Radiance Research, Seattle, WA) with a 1-μm impactor upstream of the instrument. Non-methane hydrocarbons were sampled in stainless steel canisters and measured with a GC-flame ionization detector (*38*).

Hg^0 was measured using a Tekran Inc. (Toronto, Canada) model 2537A cold vapor atomic fluorescence spectroscopy (CVAFS) instrument. In this instrument, air is pulled through a gold cartridge for 5 min to preconcentrate the Hg^0. The Hg amalgamated to the gold is then desorbed by heating and detected by CVAFS. The instrument contains two matched gold traps, which allows for continuous 5-min integrated measurements via alternating sampling. Our calibration procedure is similar to the procedures described by Landis et al. (*39*) and consists of automated calibrations every 2 d using an internal permeation source. Comparisons of the internal Hg^0 source against a primary standard Hg^0 source were made quarterly and agreed to within 5%.

At Cheeka Peak, the 2537A instrument was housed inside the main instrument trailer with a heated Teflon line (~40 °C) extending up to the sample platform at a height of 10m. During the initial phase of this work, a quartz filter was installed at the inlet (also heated to ~40 °C) to remove PHg and RGM. A soda lime trap was also present in the sampling line in order to avoid gold cartridge "passivation" by co-collected compounds (*39*). The filter and trap were replaced during each site visit—about every 2 weeks. In September 2001, a Tekran model 1130 automated speciation module was added to the system to replace the heated filter, but the soda lime trap remained in place. There was no systematic change in the measured 2537A calibration factors as a result of the 1130 installation. The 1130 system was configured to measure 4-h integrated RGM samples using a KCl-coated quartz annular denuder at 10 L/min. During the 4-h RGM sampling period, 5-min Hg^0 samples were continuously quantified by the 2537A analyzer. After the 4-h sampling period, the 1130 system was flushed with Hg-free air, and the RGM collected onto the quartz denuder was thermally decomposed into the Hg-free air and subsequently quantified as Hg^0. The method detection limits (MDL) for Hg^0 and RGM for this system configuration were 0.1 ng/m^3 and 1.6 pg/m^3, respectively (*39*).

The 24-h integrated particulate samples were collected onto prebaked 47-mm quartz fiber filters using a Rupprecht and Patashnick (Albany, NY) Dichotomous Partisol-Plus sequential sampler (model 2025). This sampler collected continuous fine fraction (<2.5 μm) and coarse fraction (2.5–10 μm) aerosols from a common airstream using a virtual impactor (*40*). A subset of quartz filters was analyzed for PHg by Frontier Geosciences (Seattle, WA) using a thermal methodology (*41*). PHg was thermally decomposed off the filters at 750 °C into Hg-free air and quantified as Hg^0 using CVAFS. PHg concentrations reported here represent the sum of the fine and coarse modes fractions, which each have an MDL of 0.2 pg/m^3.

All chemical and meteorological data were reduced to hourly averages, except the RGM measurements (every 4 h), PHg (every 24 h), and hydrocarbons (every 6 h). The scatter of the ambient signal during periods of consistent meteorology gives a standard deviation in the 2–5% range over a given 12-h period. Data were removed according to set criteria, which included successive calibrations that varied by >10% from each other, baseline deviations >5%, and warm-up periods after routine maintenance operations.

Hg^0 concentrations were also obtained from Reifel Island, a nature preserve in the Fraser River, adjacent to Vancouver, BC, Canada (*42*). This site is operated by the Canadian Atmospheric Mercury Measurement Network (CAMNet) and has been making Hg^0 measurements since 1999 with a Tekran 2357A analyzer.

Results and Discussion

Hg^0 Concentrations as a Function of Season and Air Mass Origin. Monthly mean Hg^0 concentrations for the complete (marine + continental) and marine-only segregated data sets are presented in Figure 2 for the time period May 2001–May 2002. A two-population *t*-test found that the marine data were significantly higher than the marine + continental data for all months except September, November, February,

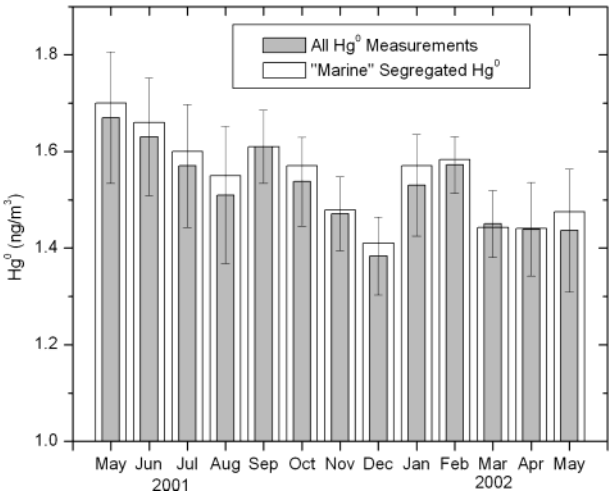

FIGURE 2. Monthly averaged concentrations of Hg^0 at CPO from May 2001 to May 2002 for marine segregated and complete data sets. Error bars represent the sample standard deviation of each month.

TABLE 1. Hg^0 Mean Concentrations by Season, Segregated into Marine and Continental Categories[a]

	[Hg^0] (ng/m³)		% difference between marine and continental
	marine	continental	
spring (May 2001, Mar−May 2002)	1.54 ± 0.16 (n = 1487)	1.46 ± 0.12 (n = 1211)	5.2
summer (Jun−Aug 2001)	1.61 ± 0.13 (n = 1379)	1.50 ± 0.13 (n = 609)	6.8
fall (Sep−Nov 2001)	1.54 ± 0.09 (n = 562)	1.49 ± 0.09 (n = 524)	2.6
winter (Dec 2001−Feb 2002)	1.51 ± 0.12 (n = 575)	1.47 ± 0.12 (n = 761)	2.6

[a] The percent differences between marine and continental means are statistically significant (p < 0.0001).

March, and April (p < 0.001). The highest monthly mean occurred in May 2001 (1.67 ng/m³), and the lowest occurred in December (1.38 ng/m³). Significant interannual variability (p < 0.0001) is apparent when means for May 2001 (1.67 ng/m³) and 2002 (1.43 ng/m³) are compared (14% difference). This difference is not likely a result of incorporating the Tekran 1130 speciation unit beginning September 2001 through May 2002, as regular internal calibrations revealed no systematic difference in response before and after installing the 1130. The lack of a clear seasonal trend in our data is different from other mid-latitude Northern Hemisphere sites, which generally show a spring maximum and an approximate amplitude of 5−20% (*14*−*16*, *42*, *43*).

Table 1 highlights the mean Hg^0 concentrations in marine and continental air. In every season, continental is lower than marine Hg^0 (p < 0.0001), with the greatest difference observed in the spring and summer. Because urban and industrial areas lie predominantly to the east of CPO, continental air containing anthropogenic pollution almost always arrives on easterly winds. Figure 3 shows wind roses for Hg^0, RGM, and CO averaged over the entire data set. CO is an ideal tracer for anthropogenic pollution as it is fairly stable (1 month lifetime) and is emitted during fossil fuel combustion. Not surprisingly, CO concentrations are much higher on easterly winds than from other directions. RGM also has predominantly industrial sources, yet its lifetime is quite short, on the order of hours to days. Although RGM concentrations are quite low from all wind directions, they are significantly higher on easterly winds (two-population t-test, p < 0.0001). Hg^0, on the other hand, shows *lower* concentrations on easterly winds, even though it also has industrial sources. This surprising result suggests removal and/or conversion to other Hg species during transit to CPO on a rapid time scale.

Our analysis focuses on anthropogenic pollution events with the largest Hg^0 concentration changes. These are shown in Figure 4A−C for summer, fall/winter, and spring, respectively. The letters A−M denote periods where CO was enhanced >5 ppbv and Hg^0 changed >0.05 ng/m³ (positive or negative) relative to the marine background. In addition to events A−M, many other spikes and dips in Hg^0 are visible in Figure 4, but because these do not meet the above-mentioned criteria for anthropogenic pollution, they will not be discussed here. Figure 4 also shows close-ups of the two types of events that will be discussed below: local pollution with Hg^0 loss and local pollution with Hg^0 enhancement. Table 2 summarizes the data for each local event (A−H and L), including concentration changes for CO, O_3, and Hg^0 averaged over the duration of the event (n = number of hours) and linear correlation coefficients between CO−Hg^0 and O_3−Hg^0. The duration of each event includes 3 h before and after concentrations deviate from the background values. Table 5 summarizes the data from the three Asian pollution events (I−K), which will be discussed below.

Local Anthropogenic Pollution Events: Hg^0 Loss in Summer. As shown in Table 2, the greatest number of Hg^0 loss events and with the largest magnitudes occurred between May 10 and August 30, labeled A−E in Figure 4A (summer) and M in Figure 4C (spring). These Hg^0 losses were accompanied by increases in CO and O_3, which produced negative correlations between CO−Hg^0 and O_3−Hg^0. The O_3−Hg^0 correlation is consistently stronger and may suggest a photochemical mechanism for Hg^0 removal, as will be discussed below.

The strongest and longest lasting Hg^0 loss event occurred August 8−13, labeled E and shown in detail in Figure 4A. This was a regional photochemical smog episode that extended over the entire western Washington and southwestern British Columbia region (*44*), producing the largest percent increases in CO and O_3 during this campaign. Hg^0 concentrations averaged 1.32 ng/m³ for these 6 d, which is significantly lower (p < 0.0001) than the summertime continental and marine averages of 1.50 and 1.61 ng/m³, respectively (Table 1). CPO back trajectories, shown in Figure 5, for August 8−11 (the most polluted days), show that air passed over the Vancouver, BC, area about 12 h prior to arriving at CPO. Using Hg^0 measurements from CAMNet at Reifel Island (*42*), we are able to speculate on the lifetime of Hg^0 in anthropogenic pollution under these meteorological conditions. The average Hg^0 concentration for August 8−11 from Reifel Island is 1.66 ng/m³, and from CPO it is 1.33 ng/m³, which is a loss of 20%. Considering that the average marine background Hg^0 concentration for this season is 1.61 ng/m³, dilution of the pollution plume with cleaner air is not expected to change the Reifel Island Hg^0 concentration significantly. Thus, as a first approximation, a simple first-order decay equation is used to determine the lifetime of Hg^0 and gives a result of 54 h. While this result is speculative, it does serve to illustrate the large potential for deposition of mercury from the atmosphere in close proximity to its sources.

The diurnal cycle of Hg^0 and O_3 during this event (Figure 6) suggests that a photochemical mechanism is responsible for such a rapid turnover in Hg^0. The concentrations of O_3 and Hg^0 at CPO for August 8−13 were negatively correlated (r = −0.53 [p < 0.01; n = 138]) and even more so between 3:00 p.m. and 6:00 a.m. local time (r = −0.65 [p < 0.01; n = 94]) when O_3 concentrations were at their daily maximum. In addition, the O_3 maximum at CPO for the entire event (60

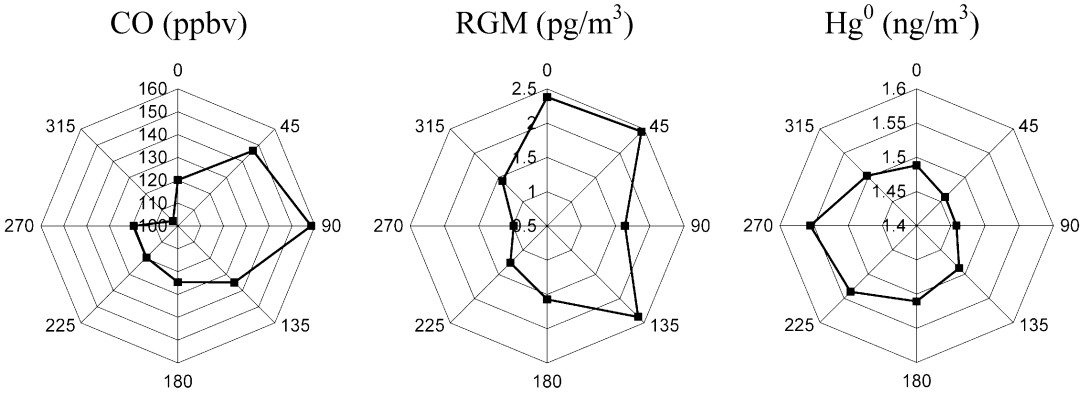

FIGURE 3. CO, RGM, and Hg^0 concentrations as a function of wind direction (in degrees) for May 2001−2002 at CPO. All marine and continental data are included.

ppbv) occurred on August 10 at 9:00 p.m., and the 22 h centered around this time gave an Hg^0-O_3 correlation of $r = -0.87$ ($p < 0.01$; $n = 22$).

The Reifel Island diurnal cycle, shown in the top panel of Figure 6, has a similar phase to the CPO cycle with a morning maximum and an evening minimum yet is about a factor of 2 larger in amplitude. If photooxidants are important in removing Hg^0, then this enhanced amplitude may reflect the very high levels of O_3 (up to 80 ppbv) that were observed in the Vancouver−Seattle area during each afternoon and evening between August 8 and August 13 (*44*). However, Kellerhals et al. (*42*) suggest that the main cause for the phase of this cycle is the summertime daily wind shift that brings higher Hg^0 from the east during the night and low Hg^0 from the west during the day. At CPO, we do not observe such a wind pattern, which argues for more of a photochemical mechanism. Between August 8 and August 10, winds at CPO were consistently from the east/northeast, and between August 11 and August 13 the winds were fairly consistently from west/southwest, with no diurnal pattern during either period.

Local Anthropogenic Pollution Events: Hg^0 Loss in Fall/Winter. During the fall/winter (Figure 4B), Hg^0 loss events become less frequent, less intense, and have the opposite relationship to O_3. Events F and H in Figure 4B are associated with decreased O_3, which results in a small positive O_3-Hg^0 correlation (Table 2). Local pollution often contains as low as 10 ppbv O_3 at this time of year owing to minimal photochemical processing and sufficient anthropogenic NO_x to quickly react with O_3. Thus, nighttime oxidants such as NO_3 may be important for removing Hg^0 (*45*) in the winter in the absence of photochemically produced oxidants such as OH that are more abundant in the summer. This hypothesis is supported by Figure 7, which shows how the average winter (December−February, $n = 761$) and summer (June−August, $n = 609$) diurnal cycles of continental segregated Hg^0 data are nearly out of phase with one another. The winter pattern shows net Hg^0 loss during the night, whereas the summer pattern shows net loss during the day, consistent with there being different removal mechanisms between the two seasons.

Local Anthropogenic Pollution Events: Hg^0 Enhancements. Although most local pollution events at CPO brought decreased Hg^0 levels, two events showed enhanced CO and Hg^0, once in the fall (Figure 4B, event G) and once in the spring (Figure 4C, event L). These events occurred near in time to Hg^0 loss events F and M and are shown in detail in Figure 4B,C. The average magnitude of Hg^0 enhancements is about the same (15% of the background) as the average loss magnitudes. While it is not immediately obvious what causes such variable behavior in Hg^0, a comparison of the average trends of enhancement and loss events in the fall, winter, and spring can provide some clues. This comparison is shown in Table 3. Average Hg^0, CO, and O_3 deviations for the events as a whole have been calculated by weighting the deviation for a single event with the duration of that event. In this way, event F (73 h [see Table 2]), for example, will have the largest effect on the average total Hg^0, CO, and O_3 deviations. What can be noticed from these data is that Hg^0 enhancement events on average are shorter-lived, have higher CO enhancements, and have slightly lower O_3 deviations as compared to Hg^0 loss events. Higher CO levels may be indicative of fresher and/or less dilute pollution, which may have contained higher Hg^0 levels at the source region in addition to decreasing the available reaction time for Hg^0 while the air parcel is en-route to CPO. If this occurs in conjunction with relatively low photochemical activity, then the likelihood of seeing an Hg^0 enhancement at CPO may be increased. O_3 deviations associated with Hg^0 enhancement events are slightly lower than during loss events; however, given the complex behavior of O_3 during all of these events in general (and event G in particular, see close-up of Figure 4B), we are hesitant to draw any firm conclusions. It is apparent, however, that the dependence of Hg^0 levels on transport and photochemistry is in contrast to previous studies that have observed Hg^0 enhancements downwind of local pollution sources under all conditions and in every season (*16*, *46*−*49*). Clearly, more measurements are needed to better resolve this discrepancy.

Reactive Mercury Species. RGM and PHg are associated with gas- and/or aqueous-phase oxidation of atmospheric Hg^0 in addition to being released directly by some anthropogenic processes. RGM measurements were made from September 2001, and PHg measurements were made during selected periods in August, March, and April. These data are presented in Table 4 as a function of season and air mass origin. The bulk of the 4-h RGM measurements are very low (<MDL) and were assigned a value of 1/2 of MDL for the purpose of calculating seasonal means. RGM from the marine sector was almost always <MDL, in contrast to the findings by Mason et al. (*5*), who report RGM levels around 300 pg/m^3 over the open ocean near Bermuda. Our PHg measurements from the marine sector averaged 0.5 pg/m^3 (Table 4), which is consistent with the results from Mason et al. (*5*).

Several local pollution events brought enhanced RGM concentrations, such as days 325, 95, 115, and 120 (Figure 4B,C), when values reached the 10−20 pg/m^3 range. These days have not been included in the analysis with the other events (A−M) because they did not satisfy both the CO enhancement and Hg^0 fluctuation criteria mentioned above. Admittedly, we do not understand why some local events (event G) would bring large CO spikes, an increase in Hg^0, and essentially no change in RGM, whereas other events (day 325) bring the largest RGM spike of the campaign and

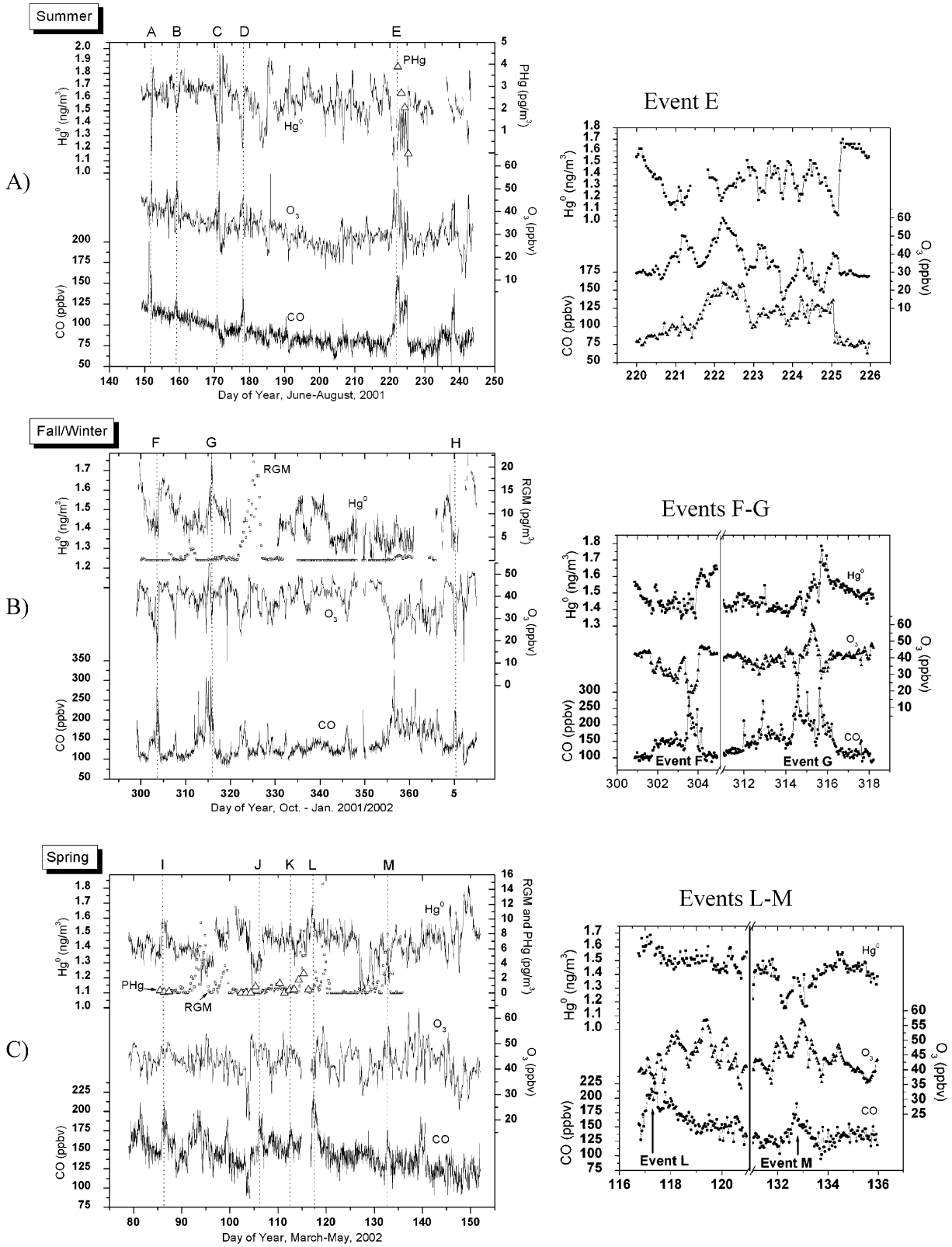

FIGURE 4. (A) Summer, (B) fall/winter, and (C) spring measurements of Hg^0, RGM, PHg, O_3, and CO with local and Asian anthropogenic pollution events highlighted by letters A−M. Close-ups of the events E−G, L, and M show comparisons between local Hg^0 loss and enhancements.

much less CO. A better understanding of RGM formation and deposition processes will hopefully help resolve this discrepancy.

During the spring of 2002 (days 95, 98, 115, 120, and 132), Hg^0 and RGM were weakly negatively correlated in continental air (see Table 4), suggesting a removal pathway for at least some of the Hg^0. The greater light levels in spring may encourage more Hg^0−RGM transformations. However, the highest RGM values we see only account for about 2% of the total Hg pool, with PHg adding another 1%. Thus, the question

TABLE 2. Summary of Local Anthropogenic Pollution Events, Categorized by Their Effect (Loss or Enhancement) on Hg^0 Concentrations[a]

event and date	*n* (h)	change compared to monthly marine mean: CO (ppbv)	O_3 (ppbv)	Hg^0 (ng/m³)	correlation coefficient (*r*): CO−Hg^0	O_3−Hg^0
Hg^0 Losses						
summer						
A, 5/31/01, day 151	12	+27	+10	−0.27	−0.45	−0.82
B, 6/7/01, day 158	29	+16	+5	−0.09	−0.48	−0.61
C, 6/19/01, day 170	37	+5	+4	−0.20	−0.31	−0.63
D, 6/26/01, day 177	47	+11	+5	−0.16	−0.61	−0.74
E, 8/8/01, day 220	138	+32	+6	−0.19	−0.47	−0.53
fall						
F, 10/28/01, day 301	73	+30	−7	−0.06	−0.12	0.47
winter						
H, 1/4/02, day 4	33	+18	−6	−0.10	−0.23	0.45
spring						
M, 5/11/02, day 131	35	+12	+6	−0.19	−0.07	−0.28
Hg^0 Enhancements						
fall						
G, 11/10/01, day 314	27	+84	+1	+0.11	0.13	−0.62
spring						
L, 4/26/02, day 116	17	+40	−2	+0.15	0.15	0.02

[a] Changes in concentrations are given as the average over the duration of the event (*n*), defined as 3 h before and after changes in Hg^0 concentrations.

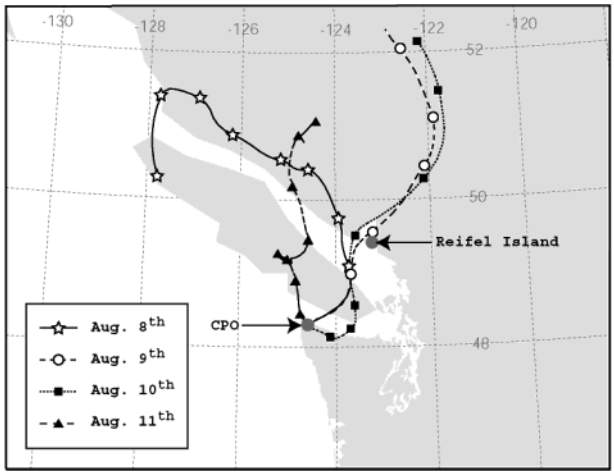

FIGURE 5. 48-h back trajectories arriving at CPO (500 m above sea level) each day during August 8−11, 2001. Arrival times are 10:00 a.m. local time. Each symbol represents 6 h back in time. Trajectories are calculated using the NOAA-HYSPLIT model (quasi-isentropic vertical motion) (http://www.arl.noaa.gov/ready/) with the EDAS (Eta Data Assimilation System) meteorological dataset (3 h time and 80 km horizontal resolution).

as to the fate of the missing Hg^0 is currently open. It is possible that Hg^0 conversion to PHg or RGM is occurring upwind, and these compounds are then removed during transit. Supporting evidence for this idea comes from our limited PHg data (Table 4), which indicate that coarse mode particles (2.5−10 μm) contain 1−3 times higher Hg concentrations compared to the fine mode (<2.5 μm). This finding is consistent with observations from the MBL on the coast of Florida (*50*). Since larger particles would generally be more susceptible to deposition and have a shorter lifetime than smaller particles, this may be an important pathway for Hg^0 removal.

Hg^0 Concentrations in Air of Asian Origin. Previously we have shown that air with significant enhancement of Asian industrial emissions can be transported across the Pacific in as little as 5 d, based on observations at CPO and from aircraft

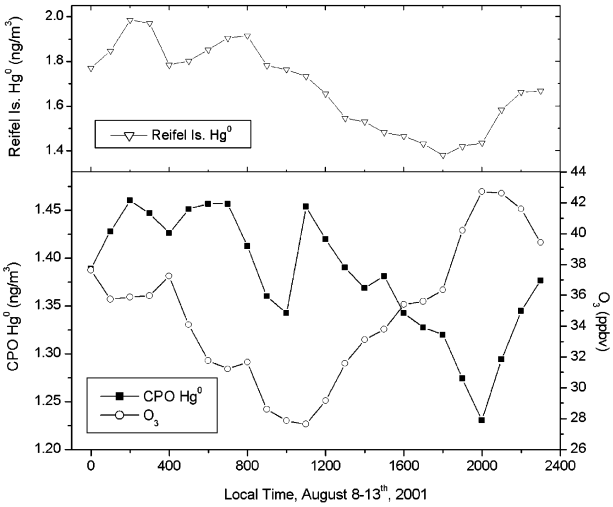

FIGURE 6. Average diurnal cycles for Hg^0 and O_3 at CPO and Hg^0 at Reifel Island, BC, for the period August 8−13, 2001.

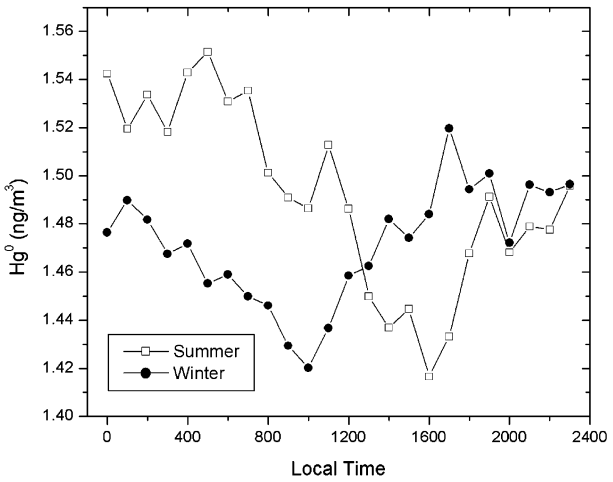

FIGURE 7. Comparison of the winter and summer diurnal cycles from continental segregated data at CPO.

TABLE 3. Comparison of Hg^0 Loss and Enhancement Events during the Fall, Winter, and Spring at CPO[a]

	avg event duration (h)	avg Hg^0 deviation (ng/m³)	avg CO deviation (ppbv)	avg O_3 deviation (ppbv)
Hg^0 losses F, H, and M	47	−0.10	+23	−3.5
Hg^0 enhancements G and L	22	+0.13	+67	−0.2

[a] Averages are time-weighted according to the duration of each individual event.

(*25*−*27*). During the spring of 2002, we identified three additional events at CPO, which are shown in Figure 4C, labeled I−K. Back trajectories from the NOAA-HYSPLIT model (*33*, *34*) and results from the GEOS-CHEM chemical tracer model (*51*) were used to confirm that these air masses had enhanced concentrations of CO due to Asian sources. Radon and particle scattering enhancements also confirmed the presence of continental sources. Average concentration changes for CO, O_3, and Hg^0 along with correlations between CO−Hg^0 and O_3−Hg^0 and propane to ethane ratios are given in Table 5.

The amount of CO enhancement during these events (15−30 ppbv) compares well to previous Asian events at

TABLE 4. Summary of RGM and PHg Concentrations by Season, Segregated into Marine and Continental Categories[a]

	marine		continental		
RGM (pg/m^3)	*n*	avg	*n*	avg	correlation with Hg^0 (*r*)[b]
fall 2001	154	<MDL	178	2.0	0.04 ($n = 10$; $p = 0.92$)
winter 2001−2002	220	<MDL	273	<MDL	0.07 ($n = 14$; $p = 0.80$)
spring 2002	227	1.6	206	2.7	−0.23 ($n = 77$; $p = 0.05$)

	marine		continental		
PHg (pg/m^3)	*n*	avg	*n*	avg	coarse/fine mode ratio[c]
summer 2001	1	<MDL	3	2.9	1.5
spring 2002	12	0.5	2	1.5	2.6

[a] *n* refers to the number of hourly averages. PHg represents the sum of the fine (<2.5 μm) and coarse (2.5−10 μm) mode fractions. [b] The correlation coefficient (*r*) with Hg^0 is calculated for 4-h averages of continental segregated data with all RGM < MDL removed. [c] Coarse/fine mode ratio includes both marine and continental PHg data.

CPO (*26*−*28*). However, the changes we observed in Hg^0 concentrations are small, which is an important result given the large mercury sources in the East Asian region (*18*). Hg^0 behavior is seemingly complicated, with a pattern not unlike what was observed during fall/winter enhancements in local pollution. Variables may include different source regions, processing times, and mechanisms between each event. For example, events I and K brought enhancements of Hg^0, while event J showed an Hg^0 loss. Event I was a particularly clear example of Asian industrial pollution, with back trajectories indicating about a 6-d transit time from northern Japan and a relatively high propane/ethane ratio (Table 5). Since propane has a much shorter lifetime (~10 d) as compared to ethane (~30 d), a higher ratio indicates fresher emissions and/or less photochemical processing en-route, consistent with the back trajectories. Event J on the other hand shows a weak CO−Hg^0 correlation and a much lower propane/ethane ratio. This suggests more aging and photochemical processing during event J and may explain the lower Hg^0 concentrations we observed.

The O_3−Hg^0 correlations during Asian events are not as consistent as during local pollution events. In particular, events I and K showed negative and positive O_3−Hg^0 correlations, respectively, even though both events brought enhanced Hg^0 and similar propane/ethane ratios. The reason for the inconsistency may be due to the complicated behavior of O_3 during long-range transport. According to Jaffe et al. (*28*), O_3 enhancements at CPO are more likely when transport occurs in the free troposphere and/or in the absence of mineral dust. The transport pathways and conditions for events I and K may have been particularly different in their effects on O_3 but not necessarily for Hg^0, propane, or ethane.

Diurnal Cycles of Hg^0 in the Marine Background. Figure 8 shows the variations in Hg^0 concentration of marine segregated data, averaged by time of day for the different seasons. The summer diurnal cycle is the most evident compared to other seasons, with a peak-to-peak variation of 7% of the average summertime concentration of 1.61 ng/m^3. The maximum during summer comes in the early morning hours, 2:00−5:00 a.m. local time, and the minimum is in the late afternoon, 3:00−6:00 p.m. Other seasons show smaller diurnal cycles, about 4%, with different phases than summer. Spring has its maximum around midnight and its minimum centered on midday. Fall shows a pattern that is nearly the inverse of summer, with an evening maximum and a morning minimum. Winter shows the noisiest pattern, with a midday maximum and a midnight minimum.

The summertime diurnal pattern was further analyzed for the effects of sunlight and temperature. By segregating the marine data in the month of June into the seven warmest, sunniest days (averaging 25 000 kJ m^{-2} d^{-1} radiation and 10.7 °C) and the seven coolest, cloudiest days (averaging 12 000 kJ m^{-2} d^{-1} radiation and 7.6 °C), a dramatic effect on the average diurnal cycles was observed, as shown in Figure 9. [Sunlight irradiance was measured on top of the Atmospheric Sciences building at the University of Washington, Seattle, and is assumed to be a close approximation of the region.] The cool, cloudy days show small (<5%) diurnal changes in O_3 and Hg^0, whereas the warm, sunny days show much larger variations, about 26% for both species. This highlights the importance of temperature and/or sunlight on Hg^0 cycling processes under relatively clean conditions.

The phase of the Hg^0 diurnal cycles from the warmest marine sector days matches very closely that from the August 8−13 event, with an evening minimum and a morning maximum. We suspect that similar sink processes may be controlling Hg^0 in both marine and continental air during the summer, namely, episodic/rapid removal by a photooxidant. One significant difference, however, is that during the pollution event of August, the warmest, sunniest days produced very low concentrations of Hg^0 (~1.3 ng/m^3) whereas in marine air masses in June, the Hg^0 daily average concentration on sunny and cloudy days was about the same (1.67 ng/m^3). A possible explanation is that the marine data may also reflect diurnal cycling in the oceanic flux.

Junge Lifetime of Hg^0. Using the equation $\tau = 0.10(\sigma/\text{mean})^{-0.74}$ (*52*, *53*), where σ in the relative standard deviation, we get a Junge lifetime for Hg^0 of 0.59 yr or 7.1 month. This calculation for our marine segregated data set gives the same result. Summer marine data gives the shortest lifetime of any season (7.7 month), and fall gives the longest lifetime (9.6 month). Thus, even though we observed considerable short-term variability for Hg^0, particularly during the summer, our results indicate that the overall lifetime is within the currently accepted range (0.5−2 yr), albeit on the low end.

Possible Cycling Mechanisms for Hg^0. Our results point to both a role for rapid photochemical oxidation of Hg^0 in the late spring and summer and rapid removal by nonphoto processes in fall/winter. These processes may not only be occurring solely in polluted air but also in the clean background as well. A possible photochemical mechanism is reaction with the OH radical (*25*), as has been suggested by Temme et al. (*24*) to explain losses of Hg^0 in Antarctica during the summer. Temme et al. (*24*) indicate that high levels of NO_x are present due to photodenitrification processes in the snowpack, which has the effect of producing enhanced levels of O_3, OH, and other oxidants. This situation may be analogous to that of CPO during local pollution events, except that the source of NO_x is urban and not natural.

Reactive halogens, which are important in MDEs in polar regions, could be potentially important oxidants for Hg^0 in the MBL of the midlatitudes based on their behavior toward O_3. These species, which include BrCl, HOBr, and BrO, react rapidly with O_3 and are thought to be responsible for large diurnal cycles of O_3 observed over the Indian Ocean (*54*). There are also known sources of chlorine from urban areas (swimming pools, water purification, cooling towers) that are strongest during the summer (*55*). Chlorine in the urban environment also has the effect of enhancing O_3 production, which is consistent with our summer observations of O_3 peaks in conjunction with Hg^0 losses (*55*). Potential removal processes for Hg^0 when only limited sunlight is available (fall/winter) could be adsorption onto particles (especially coarse mode) or oxidation by NO_3 at night (*45*).

TABLE 5. Summary of Asian Anthropogenic Pollution Events during the Spring of 2002, Categorized by Their Effect (Loss or Enhancement) on Hg^0 Concentrations[a]

		change compared to monthly marine mean			correlation coefficient (*r*)		hydrocarbons
event and date	*n* (h)	CO (ppbv)	O_3 (ppbv)	Hg^0 (ng/m^3)	CO−Hg^0	O_3−Hg^0	propane/ethane ratio
				Hg^0 Losses in Asian Pollution			
J, 4/16/02, day 106	31	+28	+4	−0.09	−0.20	−0.03	0.24
				Hg^0 Enhancements in Asian Pollution			
I, 3/27/02, day 87	33	+24	+2	+0.08	0.51	−0.54	0.37
K, 4/22/02, day 112	26	+19	+4	+0.03	0.19	0.49	0.34

[a] Changes in concentrations are given as the average over the duration of the event (*n*), defined as 3 h before and after changes in Hg^0 concentrations.

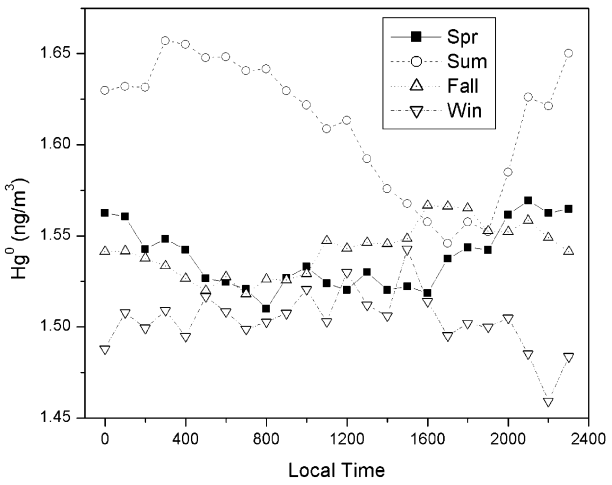

FIGURE 8. Average diurnal cycles for marine segregated data from four seasons.

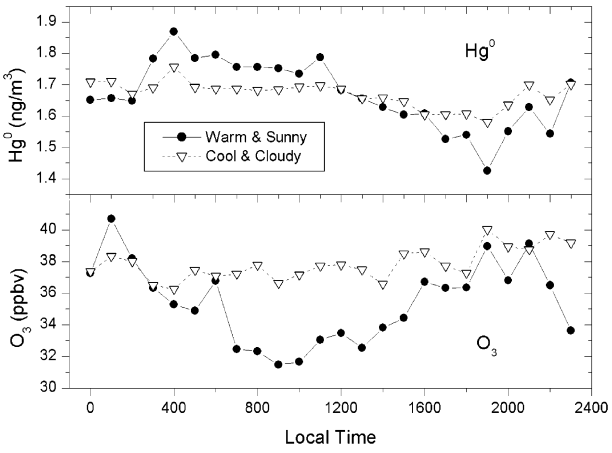

FIGURE 9. Comparison of average diurnal cycles of Hg^0 and O_3 from the seven warmest, sunniest days and the seven coolest, cloudiest days in June 2001. Marine data only.

Uptake of Hg^0 by terrestrial vegetation has been previously speculated to be the cause of lower Hg^0 levels in continental versus marine air (*49*). From the coast of the eastern Baltic Sea, in Preila, Lithuania, Urba et al. (*49*) report summertime Hg^0 concentration of 1.43 ng/m^3 from westerly (marine) winds and 1.31 ng/m^3 from easterly (continental) winds. We find no evidence of a vegetation sink in our region, since continental air that bears the same chemical signature as marine air (i.e., low CO and particle scattering) does not contain lower levels of Hg^0.

Our surprising observations of Hg^0 losses during local pollution events point to significant gaps in the understanding of Hg cycling. One possible explanation is that injection of urban emissions into the boundary layer (including particulates, O_3, and other oxidants) enhances the reactivity and reduces the Hg^0 lifetime. This would produce Hg^0 concentrations downwind of an urban area that are lower than the local background. Presumably, this would also lead to enhanced deposition of mercury, not only from local emissions but also by increasing the deposition of the global background Hg^0. Additional work is necessary to evaluate if this hypothesis is correct.

Acknowledgments

We thank the Canadian Atmospheric Mercury Measurement Network (CAMNet) and Environment Canada for providing the elemental mercury data from Reifel Island. We also thank the Makah Nation for allowing us to sample the atmosphere on their lands. Lyatt Jaegle and Qing Liang provided the GEOS-Chem results, James B. Dennison constructed the maps in this paper, and Phil Schwartzendruber provided the PHg data. This work was funded by the U.S. Environmental Protection Agency Office of International Affairs and Office of Research and Development (Cooperative Agreement X-82825001-0). It has been subjected to Agency review and approved for publication. Mention of trade names or commercial products does not constitute an endorsement or recommendation for use.

Literature Cited

(1) Wheatley, B.; Wheatley, M. A. *Sci. Total Environ.* **2000**, *259*, 23−29.
(2) Lindqvist, O.; Rodhe, H. *Tellus* **1985**, *37B*, 136−159.
(3) Schroeder, W. H.; Munthie, J. *Atmos. Environ.* **1998**, *32*, 809−822.
(4) Lin, C. J.; Pehkonen, S. O. *Atmos. Environ.* **1999**, *33*, 2067−2079.
(5) Mason, R. P.; Lawson, N. M.; Sheu, G.-R. *Deep-Sea Res., Part II* **2001**, *48*, 2829−2853.
(6) Lindqvist, O.; Johansson, K.; Aastrup, M.; Anderson, A.; Bringmark, L.; Hovsenius, G.; Håkanson, L.; Iverfeldt, Å.; Meili, M.; Timm, B. *Water Air Soil Pollut.* **1991**, *55*, 1−283.
(7) Pirrone, N.; Costa, P.; Pacyna, J. M.; Ferrara, R. *Atmos. Environ.* **2001**, *35*, 2997−3006.
(8) Mason, R. P.; Fitzgerald, W. F.; Morel, F. M. M. *Geochim. Cosmochim. Acta* **1994**, *58*, 3191−3198.
(9) Bergan, T.; Gallardo, L.; Rodhe, H. *Atmos. Environ.* **1999**, *33*, 1575−1585.
(10) Lamborg, C. H.; Fitzgerald, W. F.; O'Donnell, J.; Torgersen, T. *Geochim. Cosmochim. Acta* **2002**, *66*, 1105−1118.
(11) Schuster, P. F.; Krabbenhoft, D. P.; Naftz, D. L.; Cecil, L. D.; Olson, M. L.; Dewild, J. F.; Susong, D. D.; Green, J. R.; Abbott, M. L. *Environ. Sci. Technol.* **2002**, *36*, 2303−2310.
(12) Mukherjee, A. B.; Melanen, M.; Ekqvist, M.; Verta, M. *Sci. Total Environ.* **2000**, *259*, 73−83.
(13) U.S. EPA. EPA-452/R-97-004; 1997. Available at http://www.epa.gov/ttn/uatw/112merc/mercury.html.
(14) Slemr, F.; Scheel, H. E. *Atmos. Environ.* **1998**, *32*, 845−853.
(15) Iverfelt, Å.; Munthe, J.; Brosset, C.; Pacyna, J. *Water Air Soil Pollut.* **1995**, *80*, 227−233.
(16) Ebinghaus, R.; Kock, H. H.; Coggins, A. M.; Spain, T. G.; Jennings, S. G.; Temme, C. *Atmos. Environ.* **2002**, *36*, 5267−5276.
(17) Blanchard, P.; Froude, F. A.; Martin, J. B.; Dryfhout-Clark, H.; Woods, J. T. *Atmos. Environ.* **2002**, *36*, 3735−3743.

(18) Wang, Q.; Shen, W.; Ma, Z. *Environ. Sci. Technol.* **2000**, *34*, 2711−2713.
(19) Streets, D. G.; Waldhoff, S. T. *Atmos. Environ.* **2000**, *34*, 363−374.
(20) Pacyna, E. G.; Pacyna, J. M. *Water. Air Soil Pollut.* **2002**, *137 (1−4)*, 149−165.
(21) Lindberg, S. E.; Brooks, S.; Lin, C. J.; Scott, K. J.; Landis, M. S.; Stevens, R. K.; Goodsite, M.; Richter, A. *Environ. Sci. Technol.* **2002**, *36*, 1245−1256.
(22) Ebinghaus, R.; Kock, H. H.; Temme, C.; Einax, J. W.; Lowe, A. G.; Richter, A.; Burrows, J. P.; Schroeder, W. H. *Environ. Sci. Technol.* **2002**, *36*, 1238−1244.
(23) McElroy, C. T.; McLinden, C. A.; McConnell, J. C. *Nature* **1999**, *397*, 338−341.
(24) Temme, C.; Einax, J. W.; Ebinghaus, R.; Schroeder, W. H. *Environ. Sci. Technol.* **2003**, *37*, 22−31.
(25) Sommar, J.; Gardfeldt, K.; Stromberg, D.; Feng, X. *Atmos. Environ.* **2001**, *35*, 3049−3054.
(26) Jaffe, D. A.; Anderson, T.; Covert, D.; Kotchenruther, R.; Trost, B.; Danielson, J.; Simpson, W.; Berntsen, T.; Karlsdottir, S.; Blake, D.; Harris, J.; Carmichael, G.; Uno, I. *Geophys. Res. Lett.* **1999**, *26*, 711−714.
(27) Jaffe, D. A.; Anderson, T.; Covert, D.; Trost, B.; Danielson, J.; Simpson, W.; Blake, D.; Harris, J.; Streets, D. *J. Geophys. Res.* **2001**, *106*, 7449−7461.
(28) Jaffe, D. A.; McKendry, I.; Anderson, T.; Price, H. *Atmos. Environ.* **2003**, *37*, 391−404.
(29) Anderson, T. L.; Covert, D. S.; Wheeler, J. D.; Harris, J. M.; Perry, K. D.; Trost, B. E.; Jaffe, D. A. *J. Geophys. Res.* **1999**, *104*, 26793−26807.
(30) Washington Department of Ecology. Publication 02-03-042; Available at http://www.ecy.wa.gov/pubs/0203042.pdf.
(31) Bloom, N. S.; Prestbo, E. M.; Tokos, J. S.; Kuhn, E. S.; von der Geest, E. J. Distribution of Mercury Species in the Pacific Northwest Atmosphere. Presented at the Mercury Deposition and Cycling Symposium, 210th ACS Meeting, 1995.
(32) Harris, J. M.; Tans, P. P.; Dlugokencky, E. J.; Masarie, K. A.; Lang, P. M.; Whittlestone, S.; Steele, L. P. *J. Geophys. Res.* **1992**, *97*, 6003−6010.
(33) Draxler, R. R.; Hess, G. D. *Description of the Hysplit_4 modeling system*; NOAA Tech Memo ERL ARL-224; December 24, 1997.
(34) Available at http://www.arl.noaa.gov/ready/.
(35) Jaffe, D.; Price, H.; Parrish, D.; Goldstein, A.; Harris, J. Increasing background ozone during spring on the west coast of North America. *Geophys. Res. Lett.* **2003**, *30* (12), 1613; doi: 10.1029/200GL017024.
(36) Jaffe, D. A.; Yurganov, L. N.; Pullman, E.; Reuter, J.; Mahura, A.; Novelli P. C. *J. Geophys. Res.* **1998**, *103*, 1493−1502.
(37) Whittlestone, S. E.; Schery, S. D.; Li, Y.; *J. Geophys. Res.* **1996**, *101*, 14787−14794.
(38) Price, H. U.; Jaffe, D. A.; Doskey, P. V.; McKendry, I.; Anderson, T. L. *J. Geophys. Res.* (in press).
(39) Landis, M. S.; Stevens, R. K.; Schaedlich, F.; Prestbo, E. M. *Environ. Sci. Technol.* **2002**, *36*, 3000−3009.
(40) Poor, N.; Clark, T.; Nye, L.; Tamanenini, T. *Atmos. Environ.* **2002**, *36*, 3289−3298.
(41) Lu, J. Y.; Schroeder, W. H.; Berg, T.; Munthe, J.; Schneeberger, D.; Schaedlich, F. *Anal. Chem.* **1998**, *70*, 2403−2408.
(42) Kellerhals, M.; Beauchamp, S.; Belzer, W.; Blanchard, P.; Froude, F.; Harvey, B.; McDonald, K.; Pilote, M.; Poissant, L.; Puckett, K.; Schroeder, B.; Steffen, A.; Tordon, R. *Atmos. Environ.* **2003**, *37*, 1003−1011.
(43) Poissant, L. *Atmos. Environ.* **1999**, *33*, 2537−2547.
(44) Snow, J. A.; Dennison, J. B.; Jaffe, D. A.; Price, H. U.; Vaughan, J. K.; Lamb, B. *Atmos. Environ.* (in press).
(45) Sommar, J.; Hallquist, M.; Ljungström, E.; Lindqvist, O. *J. Atmos. Chem.* **1997**, *27*, 233−247.
(46) Poissant, L. *Sci. Total Environ.* **2000**, *259*, 191−201.
(47) Vette, A. F.; Landis, M. S.; Keeler, G. J. *Environ. Sci. Technol.* **2002**, *36*, 4525−4532.
(48) Lindberg, S. E.; Stratton, W. J. *Environ. Sci. Technol.* **1998**, *32*, 49−57.
(49) Urba, A.; Kvietkus, K.; Marks, R. *Sci. Total Environ.* **2000**, *259*, 203-210.
(50) Malcom, E. G.; Keeler, G. J.; Landis, M. S. The effects of the coastal environment on the atmospheric mercury cycle. *J. Geophys. Res.* **2003**, *108* (D12), art. 4357.
(51) Jaegle, L.; Jaffe, D.; Price, H. U.; Weiss-Penzias, P.; Palmer, P. I.; Evans, M. J.; Jacob, D. J.; Bey, I. *J. Geophys. Res.* (in press).
(52) Junge, C. E. *Air Chemistry and Radioactivity*; Academic Press: New York, London: 1963.
(53) Colman, J. J.; Blake, D. R.; Rowland, F. S. *Science* **1998**, *281*, 392−396.
(54) Dickerson, R. R.; Rhoads, K. P.; Carsey, T. P.; Oltmans, S. J.; Burrows, J. P.; Crutzen, P. J. *J. Geophys. Res.* **1999**, *104*, 21,-385−21,395.
(55) Chang, S.; McDonald-Buller, E.; Kimura, Y.; Yarwood, G.; Neece, J.; Russell, M.; Tanaka, P.; Allen, D. *Atmos. Environ.* **2002**, *36*, 4991−5003.

Received for review February 6, 2003. Revised manuscript received May 19, 2003. Accepted June 3, 2003.

ES0341081